Mesenchymal calcium waves underpin intestinal smooth muscle differentiation

Nicolas R. Chevalier, Léna Zig, Anthony Gomis, Richard Amedzrovi Agbesi, Laetitia Pontoizeau, Isabelle Eude-Le Parco, Nathalie Rouach, Isabelle Arnoux, Pascal de Santa Barbara, Sandrine Faure

Mesenchymal calcium waves underpin intestinal smooth muscle differentiation

Nicolas R. Chevalier[1*], Léna Zig[1], Anthony Gomis[1], Richard J. Amedzrovi[1], Laetitia Pontoizeau[2], Isabelle Le Parco[3], Nathalie Rouach[4], Isabelle Arnoux[4], Pascal de Santa Barbara[5], Sandrine Faure[5]

1 *Laboratoire Matière et Systèmes Complexes, Université Paris Cité, CNRS UMR 7057, 10 rue Alice Domon et Léonie Duquet, 75013 Paris, France*

2 *ANIMALLIANCE, Insourcing Department, Paris, France*

3 *Université Paris Cité, CNRS, Institut Jacques Monod, 75013 Paris, France*

4 *Neuroglial Interactions in Cerebral Physiology and Pathologies, Center for Interdisciplinary Research in Biology, Collège de France, CNRS, INSERM, Labex Memolife, Université PSL, Paris, France*

5 *PhyMedExp, University of Montpellier, INSERM, CNRS, Montpellier, France*

*Correspondence should be addressed to: nicolas.chevalier@u-paris.fr

Corresponding Author ORCID: 0000-0002-9713-1511

Abstract

Intestinal smooth muscle differentiation is a complex physico-biological process involving several different pathways. Here, we reveal using GCamp6f expressing mouse embryos that calcium waves propagate in the mouse intestinal mesenchyme one day prior to the emergence of α-smooth muscle actin in the presumptive circular and longitudinal smooth muscle layers. We find that L-type calcium channel blockers and myosine light-chain kinase inhibitors halt these waves, inhibit smooth muscle differentiation and intestinal growth. We demonstrate that the effect of the calcium waves on differentiation are not mediated via mechanobiological pathways related to smooth muscle contractions. We recapitulate most of these results in the avian embryo, and show that early guts treated with L-type channel blockers up-regulate the LIX1 factor characteristic of mesenchymal stemness, whereas older guts display KIT expressing cells characteristic of Interstitial Cells of Cajal. We conclude that electrical connectivity of the mesenchyme precedes contractile function in intestinal development and that calcium waves are required for the differentiation of mesenchymal progenitors into contractile smooth muscle cells.

Introduction

Gut motility is characterized by coordinated contractions of the intestinal smooth muscle cells (SMCs). Digestive SMCs derive from the embryonic mesoderm that gives rise to the mesenchyme, which in turn differentiates into submucosa, KIT-positive interstitial cells of Cajal (ICCs), and smooth muscle cells (SMCs) (Le Guen et al., 2015; Wallace and Burns, 2005). Digestive mesenchymal progenitors are defined by the expression of the LIX1 gene (McKey et al., 2016). Their differentiation into SMCs

requires the induction of *MYOCD*, a master regulator of SMC-restricted gene expression. Determined SMCs are defined by the early expression of the alpha and gamma isoforms of smooth muscle actin (respectively αSMA and γSMA). Later during development, SMCs organize in smooth muscle layers and express proteins involved in contractility, such as CALPONIN and SM22. Smooth Muscle organization in the gut is largely conserved in species as phylogenetically distant as hydra and humans (Shimizu et al., 2004). The SM is comprised of an inner circular smooth muscle (CSM) layer, an outer longitudinal smooth muscle (LSM) layer and, depending on species, a further thin circular and/or longitudinal layer located below the epithelium called the muscularis mucosae. The CSM and LSM are the essential effectors of bulk bolus motion by peristalsis (Amedzrovi Agbesi and Chevalier, 2021) or segmentation (Huizinga et al., 2014), while the muscularis mucosae drives smaller scale motion of epithelial villi and of the lymph vessels circulating within them.

The most important signaling pathways involved in CSM differentiation are the Sonic Hedgehog (Shh) and Bone Morphogenetic Protein pathways (BMP). Modulation of these pathways have been shown to result in strong alterations of CSM genesis, from complete disappearance (Mao et al., 2010; Ramalho-Santos et al., 2000) to hypertrophy (de Santa Barbara et al., 2005; Huycke et al., 2019) and misalignement (Sicard et al., 2022; Yang et al., 2021). Concerning the LSM, the Platelet-Derived Growth Factor (PDGF) pathway is critical because its inhibition leads to disappearance of the LSM in mice (Kurahashi et al., 2008).

It is now well understood that the emergence of smooth muscle depends not only on intrinsic factors, but also on mechanical tensile stress acting within the gut tissue: internal circumferential tension due to rapid proliferation of the epithelium causes the first SM layer to orient circularly (Huycke et al., 2019). Spontaneous contractions of this first layer generate cyclic circumferential compression and longitudinal tension that orients the second layer longitudinally (Chevalier, 2022; Chevalier et al., 2021a): halting contractions during CSM layer formation inhibits alignment of the LSM layer in the chicken embryo (Huycke et al., 2019).

Recently, the bioelectrical events underlying differentiation and morphogenesis of organs has attracted much attention (George and Bates, 2022). It is becoming clear that the polarization state of the cell (membrane potential), the electric connectivity between groups of cells (gap junctions), and their ability to propagate coordinated signals like calcium waves (Uhlén and Fritz, 2010), all play important roles in development. Thus the epithelium of the wing of the D. Melanogaster embryo spontaneously generates calcium waves and disruption of this wave pattern leads to abnormal wing development (Brodskiy et al., 2019). Calcium oscillations have been detected in the developing chicken feather buds and found to play a critical role in their morphogenesis (Li et al., 2018). Chondrogenesis in the mouse limb bud has been shown (Atsuta et al., 2019) to be preceded by a depolarization event that induces calcium transients mediated by the L-type calcium channel $Ca_v1.2$; perturbations of the physiological electric pattern led to abnormal limb growth.

Here, we show using a genetically modified mouse line expressing the fluorescent reporter GCamp6f that L-type calcium channel sensitive calcium waves propagate in the mesenchyme one day prior to smooth muscle differentiation. L-type channel antagonists block smooth muscle differentiation and gut growth. We demonstrate that the effect of the calcium waves on differentiation is not mediated by the potential contractile force it can exert on the tissue. We recapitulate most of these results in the avian embryo, and show that early guts treated with L-type channel blockers up-regulate the LIX1 factor characteristic of mesenchymal stemness, whereas older guts display KIT expressing cells characteristic of Interstitial Cells of Cajal.

Results

Calcium waves propagate in the mouse gut mesenchyme before smooth muscle differentiation

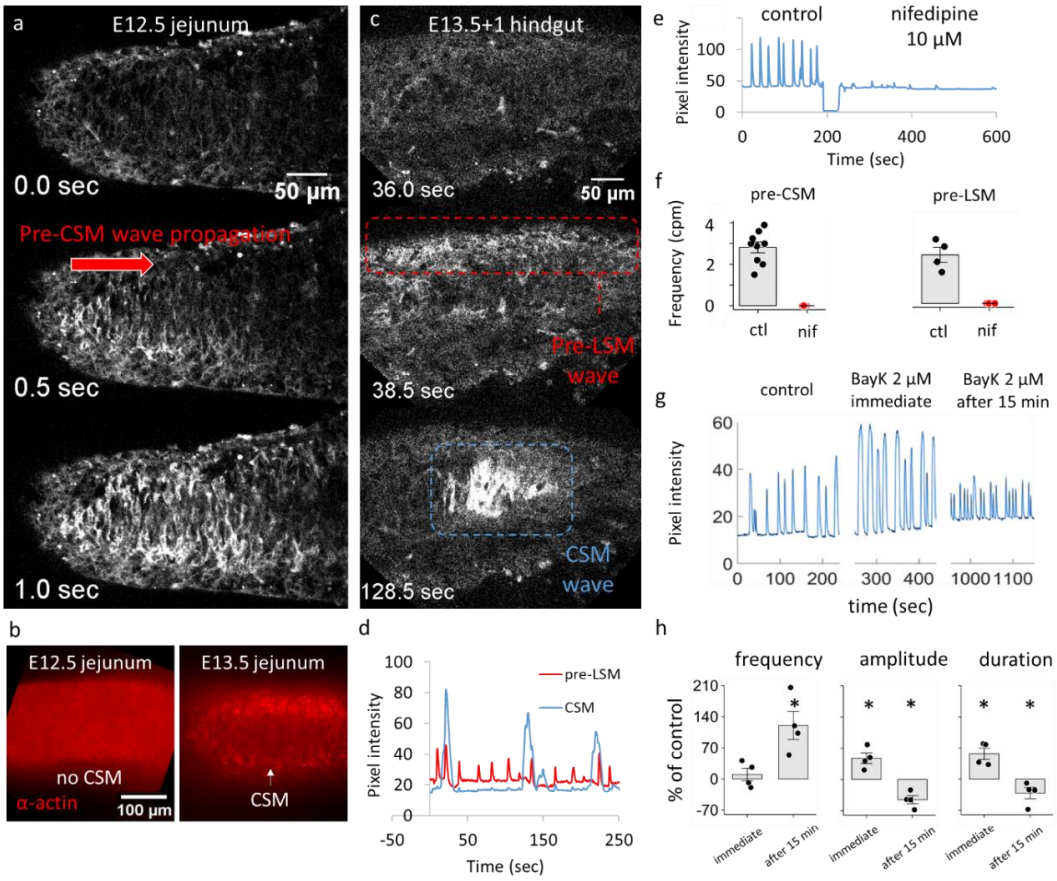

Figure 1. ***L-type channel dependent mesenchymal calcium waves are observed before α-smooth muscle actin expression in the presumptive circular and longitudinal smooth muscle layers.*** *(a) Still shots from time-lapse Video S1 showing the resting state of the E12.5 gut (top panel), and propagation (middle and bottom panels) of a calcium wave in the presumptive CSM layer. (b) Whole-mount immunohistochemistry shows that the first αSMA positive fibers appear at E13.5, the signal at E12.5 is homogeneous and non-specific. (c) Still shots from time-lapse Video S2 showing the resting state of the E13.5+1 gut (top panel), a pre-LSM wave at the gut periphery (middle panel), and a CSM wave in the center of the gut (bottom panel). (d) Pre-LSM and CSM waves at E13.5+1 (Video S3) have distinct temporal patterns. (e) Nifedipine inhibition of midgut E12.5 pre-CSM calcium waves (Video S1), (f) confirmed on n=4 samples. (g) Calcium signal of E12.5 gut: control, immediately after BayK (2 µM) application, and after 15 min application. (g,h) Effect of BayK on the frequency, amplitude and duration of E12.5 midgut pre-CSM calcium waves, as % of control, n=4. *: statistically significant p<0.05, Student t-test.*

α-smooth muscle actin (α-SMA) positive CSM fibers can first be detected in the mouse at stage E13.5 in the midgut and at E14.5 in the hindgut (Chevalier et al., 2021b; McHugh, 1995; Roberts et al., 2010). α-SMA expression corresponds with the time at which the first spontaneous motility (contractile) events can be observed in the gut (Chevalier et al., 2021b; Roberts et al., 2010). These early contractile events are purely myogenic and mediated by calcium waves that propagate across gap-junctions in the smooth muscle syncytium (Chevalier, 2018). The propagation of calcium waves has been reported in the E4 chicken gut (Huycke et al., 2019), before smooth muscle differentiation. We similarly observed that spontaneous propagating calcium waves were present at E12.5 in the mouse gut (Fig.1a, Video S1), 1 day prior to differentiation of the CSM (Fig.1b). Calcium waves at this stage did not result in any contraction or movement of the samples. These waves propagated either in the rostro-caudal or caudo-rostral direction, had an average frequency of 2.8 ± 0.4 cpm (*n*=9) and speed of 356 ± 49 µm/sec

(*n*=9). The speed of pre-CSM waves was significantly higher than the speed of CSM waves at E14.5, which was always comprised between 10 and 100 µm/sec (*n*=4); the intensity ratio (peak over baseline) of the pre-CSM waves ranged between 1.2 and 4.5, and was distinctly higher in the more rostral parts of the gut, consistent with the fact that CSM differentiation in the mouse takes place rostro-caudally. We could not detect any calcium waves in E11.5 guts, but noticed an intense bioelectric calcium activity in the budding cecum (Video S2, *n*=2). At later stages (E13.5+1 = E13.5 plus one day of culture), we detected pre-LSM waves (Fig.1c, middle panel, VideoS3). These waves could easily be distinguished from CSM waves (Fig.1c, lower panel), and had a distinct temporal pattern (Fig.1d). Both pre-CSM and pre-LSM waves were completely abolished when the L-type channel blocker nifedipine (10 µM) was applied (Fig1.e,f, Video S1). In more rostral parts of E13.5+1 (*n*=4) or E14.5 guts (*n*=4), pre-LSM activity was present as calcium "chirping", with individual elongated cells blinking asynchronously at the gut periphery (Video S4). This chirping was also extinguished after nifedipine application (*n*=4). The L-type channel agonist (S)-(−)-Bay K8644 (2 µM) significantly increased the amplitude and duration of pre-CSM waves upon application (Fig.1g,h). This pattern was followed after 15 min application by a significant rise in the frequency of waves but presenting a significantly lower, and decreasing amplitude (Fig.1g,h). We further observed *n*=2 samples 3h after BayK treatment, which presented significantly lower wave frequencies than controls at 0.1 and 0.25 cpm respectively. These observations suggest that the stimulation induced by Bay K8644 was only transitory.

L-type channel blockers inhibit smooth muscle differentiation and gut growth

We wondered how inhibition of mesenchymal calcium waves by nifedipine or nicardipine would affect gut development and smooth muscle differentiation. The choice of nifedipine or nicardipine for a given set of experiments was a matter of convenience, both blockers having similar potency (Opie, 1997). We first measured the fraction of length covered by CSM (see Materials and Methods) after culture of E12.5 guts for 3 days with nifedipine or vehicle alone (control). 10 µM nifedipine significantly reduced the extent of CSM differentiation from 80±16 % (*n*=7) to 11±7 % (*n*=8) (Fig.2a,b),whereas lower concentrations did not have a statistically significant effect. In addition to its effect on SM differentiation, the enteric nervous system of the samples was also affected, as Tuj positive cells were more scarce and did not display the physiological mesh geometry of this nerve network present in control samples (Fig.2b). We next assessed the effect of L-type calcium channel blockers on the extent of LSM coverage by culturing guts one day later, as from E13.5, for 3 days. Nicardipine 10 µM completely abolished LSM differentiation in all samples examined (Fig.2d,f) compared to controls (Fig.2d,e). The ENS was similarly altered (Fig.S1) as in E12.5+3, but the already differentiated CSM layer was unaffected (Fig.2f, Fig.S1).

The elongational growth (Fig.2g) of E13.5+3 control samples (+28 ± 18%, *n*=6) was impeded by 10 µM nicardipine treatment (-8 ± 7%, *n*=6), as was motility (Fig.2h). Interestingly, when pooling together the *n*=23 samples from this nicardipine dose-experiment, we find an almost one-to-one correlation between the presence of motility and the occurrence of growth (Fig.2i).

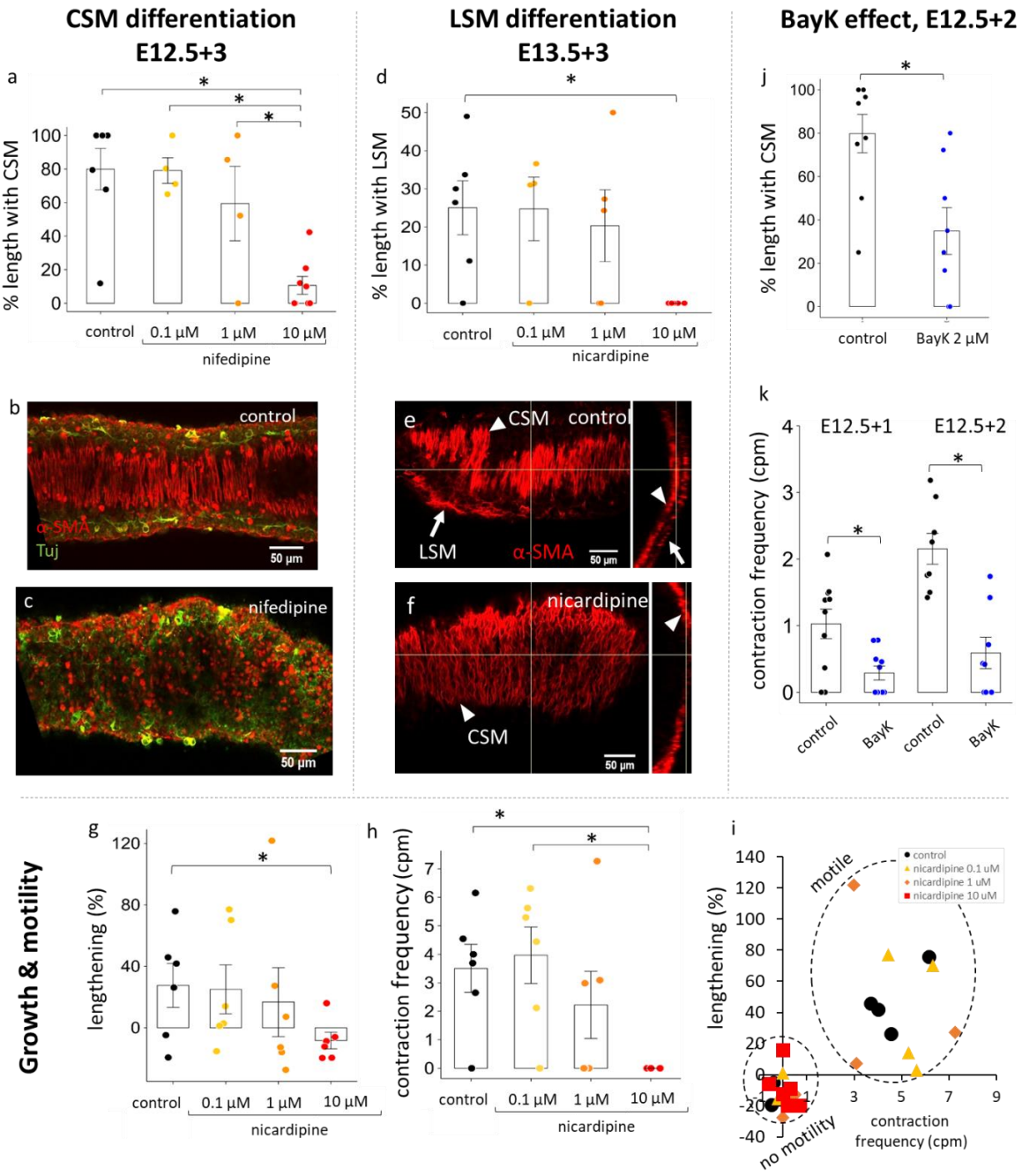

*Figure 2. **Smooth muscle differentiation can be inhibited by modulating L-type calcium channel activity.** (a) Fraction length of mouse E12.5+3 covered by CSM for control (DMSO vehicle alone 1:1000) and a range of nifedipine concentrations. (b,c) Example confocal z-slice of control and nifedipine 10 µM-treated midgut samples. (d) Fraction length of mouse E13.5+3 covered by LSM for control and a range of nicardipine concentrations. (e,f) Example confocal z-slice of control and nicardipine 10 µM-treated midgut samples. Panels on the right are orthogonal views showing the presence of an outer LSM muscle layer in controls (arrow) and its absence in the nicardipine-treated sample. (g) Length increase of E13.5+3 mouse gut compared to before culture at E13.5 for a range of nicardipine concentrations. (h) Midgut contraction frequency of E13.5+3 mouse gut for a range of nicardipine concentrations. (i) Correlation between the absence (small dashed circle) or presence (large dashed oval) of motility and growth. (j) Fraction length of mouse E12.5+2 covered by CSM for control and 2 µM BayK 8644. (k) Motility development assessed by the contraction frequency for control and 2 µM BayK 8644 treated samples. * p<0.05, Mann-Whitney two-tailed test. Each dot represents a different sample.*

We next assessed how the L-type channel agonist BayK 8644 affected CSM differentiation. We found that BayK treatment at E12.5 led to a significant reduction of CSM coverage at E12.5+2 (Fig.2j), from 80±13% (controls, *n*=9) to 35±15% (BayK, *n*=8). This result was further corroborated by the fact that

the contraction frequency of the BayK treated samples were significantly lower than controls at both E12.5+1 and E12.5+2 (Fig.2k). At day 1, only *n*=2/10 samples lacked motility in the control group, but *n*=5/10 in the BayK group; at day 2, all control samples featured motility, while *n*=3/10 still did not display any motility. CSM differentiation in the hindgut was present in *n*=5/10 controls, but in none of the BayK treated samples. No LSM could be detected at E12.5+2 in the control or BayK treated samples.

The effect of L-type channel blocking on CSM-LSM differentiation and growth could be recapitulated in another species, the chicken. Nicardipine strongly decreased CSM coverage in E5 chicken embryonic guts cultured for 3 days (Fig.S2a-c), altered the morphology of the ENS (Fig.S2c), and inhibited elongational growth of the midgut, hindgut and caeca (Fig.S2d-f). Nicardipine also inhibited LSM differentiation in E10 guts cultured for 3 days (Fig.S2h-j).

Smooth muscle differentiation is not mediated by mechanical tension

It has been demonstrated in chicken that internal mechanical strains play a major role in orienting the SM layers (Huycke et al., 2019), and perhaps also in promoting the differentiation of mesenchymal progenitors. Small tensile forces exerted by the differentiating smooth muscle could exert a positive feedback on the expression of α-actin, priming SM determination and driving further differentiation. In order to determine whether the observed inhibitory effects of L-type calcium channel blockers were due to a direct effect of the calcium waves, or were mediated via the inhibition of mechanical contraction forces induced by the calcium waves, we strived to pharmacologically dissociate these two components, i.e., to preserve the calcium waves while inhibiting contractility. Contractility in smooth muscle depends on two main pathways, the Ca^{2+} channel-calmodulin-MLCK pathway and the RhoA-Rho kinase – MLCP pathway (Deng et al., 2012). They jointly lead to phosphorylation of MLC20 that initiates contraction.

We first tested ML-7, a MLCK inhibitor downstream of calmodulin activation by Ca^{2+}. We found that ML-7 had a significant effect on the frequency of pre-CSM calcium waves as from 5 µM (Fig.3a). At 10 µM and 50 µM, the highly-synchronized physiological calcium waves became uncoordinated. Whereas in controls all cells along the diameter in the field of view would light up simultaneously, *n*=2/5 samples at 10 µM and *n*=5/5 at 50 µM showed an erratic propagation, with cells along the diameter not lightning up simultaneously (Fig.3c, Video S5), and a strongly decreased propagation speed of 24 ±10 µm/sec (*n*=7) compared to controls (356 ± 49 µm/sec). After 20 min in ML-7 50 µM, all calcium activity vanished in the gut (Fig.3a,b). ML-7, although it acts downstream of the intracellular calcium increase, perturbed the calcium handling chain in the intestinal smooth muscle cells. In culture at E12.5+2, we found that ML-7 concentrations of 10 µM and higher led to organ death (guts were dark and opaque in transmitted light, without any tissue texture), we therefore restrained the applied concentrations to 1 and 5 µM. ML-7 5 µM led to a significant decrease of CSM coverage (Fig.3d), but, unlike nifedipine, did not perturb the ENS network (Fig.S3). Although these experiments with ML-7 did not allow us to separate calcium waves from contractility, they provide a second, independent compound that linked calcium waves and/or contractility to CSM differentiation.

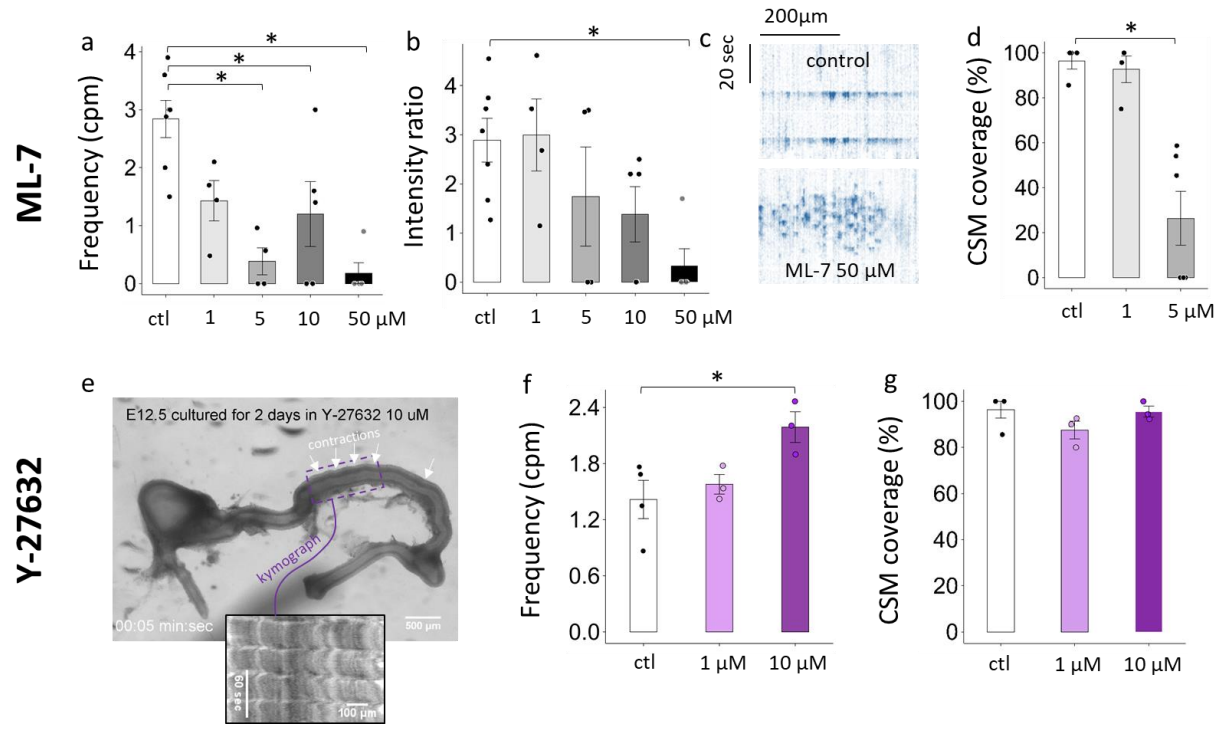

Figure 3. ***ML-7 perturbs calcium waves and Y-27632 is ineffective at inhibiting contractility****. (a) Freauency and (b) intensity ratio changes induced by ML-7 on pre-CSM calcium waves at E12.5; the effects of the highest dose (50 uM) are reported 20 min after application. (c) Kymograph of control calcium wave and wave disorganization induced by ML-7 50 µM (Video S3). (d) Effect of ML-7 on CSM coverage at E12.5+2; higher doses of ML-7 were lethal in culture. (e) E12.5+2 gut cultured in Y-27632 gut showing prominent contractile waves (white arrowheads), inset: kymograph of the red dashed region showing periodic contractions. (f) Contractile wave frequency and changes induced by Y-27632, (g) CSM coverage of E12.5+2 guts cultured in Y-27632.*

We next tested the inhibitor Y-27632, which acts on the Rho pathway. We found that Y-27632 did not have any inhibitory effect on intestinal motility at E12.5+2 (Fig.3e-g); in fact the contraction frequency of samples treated with 10 µM Y-27632 was higher than that of controls (Fig.3f). We did not investigate the effect of Y-27632 on calcium transients, but contractile waves are necessarily associated to calcium waves, that were therefore not inhibited by this compound. We raised Y-27632 to 50 µM for 1 hour, without any effect on the frequency or amplitude of propagation of contractile waves in the gut (Video S6). This indicates that the Rho pathway does not play a role in mediating contractile waves in the embryonic gut, and consequently does not affect the underlying calcium waves. Consistent with these observations, we found that Y-27632 did not affect CSM coverage in E12.5+2 guts (Fig.3g).

Because pharmacological treatment with ML-7 or Y-27632 did not provide a mean to separate calcium waves from contractility, we strived to alter the mechanical state of the gut while inhibiting calcium waves. The main mechanical strain acting at the pre-CSM stage is the circumferential residual strain (Chevalier, 2022; Huycke et al., 2019). We wondered whether nifedipine could perhaps modify this residual strain. We found that 4 hour nifedipine treatment did not affect the opening angle relative to controls (Fig.4a): both ring groups opened up to ~130°, i.e. circumferential strain of similar magnitude was present in both sample groups. This is consistent with the fact that the circumferential residual strain is due mainly to epithelial proliferation (Huycke et al., 2019). We conducted this experiment at the CSM stage E13.5 to magnify any potential effects of nifedipine; since CSM is not present at E12.5, we do not expect nifedipine to have any effect on the opening angle at E12.5. At the pre-LSM stage, the main mechanical stress is the longitudinal strain component (Poisson-effect) associated to CSM contractions (Chevalier, 2022; Chevalier et al., 2021a; Huycke et al., 2019). We therefore set-up an experiment (inset Fig.4b, Video S5, Materials and Methods) to simulate this longitudinal strain, while

keeping the intestines in culture in nifedipine for 2 days (between E14.5 and E14.5+2). Longitudinal cyclic stretch amplitude was 5-10% and was applied at a frequency of 1 cpm, similar to the physiological contraction magnitude in the embryonic gut at these stages (Chevalier et al., 2021b). The stretch applied was sufficient to viscoelastically elongate the guts, which had to be repositioned regularly to continuously apply a longitudinal stress (cf Materials & Methods). We found that whereas control guts showed a high degree of LSM differentiation (58 ± 9 %, *n*=8), the LSM coverage of cyclically stretched guts in nifedipine was extremely low (6 ± 4 %, *n*=4, Fig.4b) and not different from control guts kept in nifedipine without stretch (11 ± 5%, *n*=7, Fig.4b). This suggests that the effect of the calcium waves on smooth muscle differentiation is not mediated via the contractile force it can potentially exert on the mesenchyme.

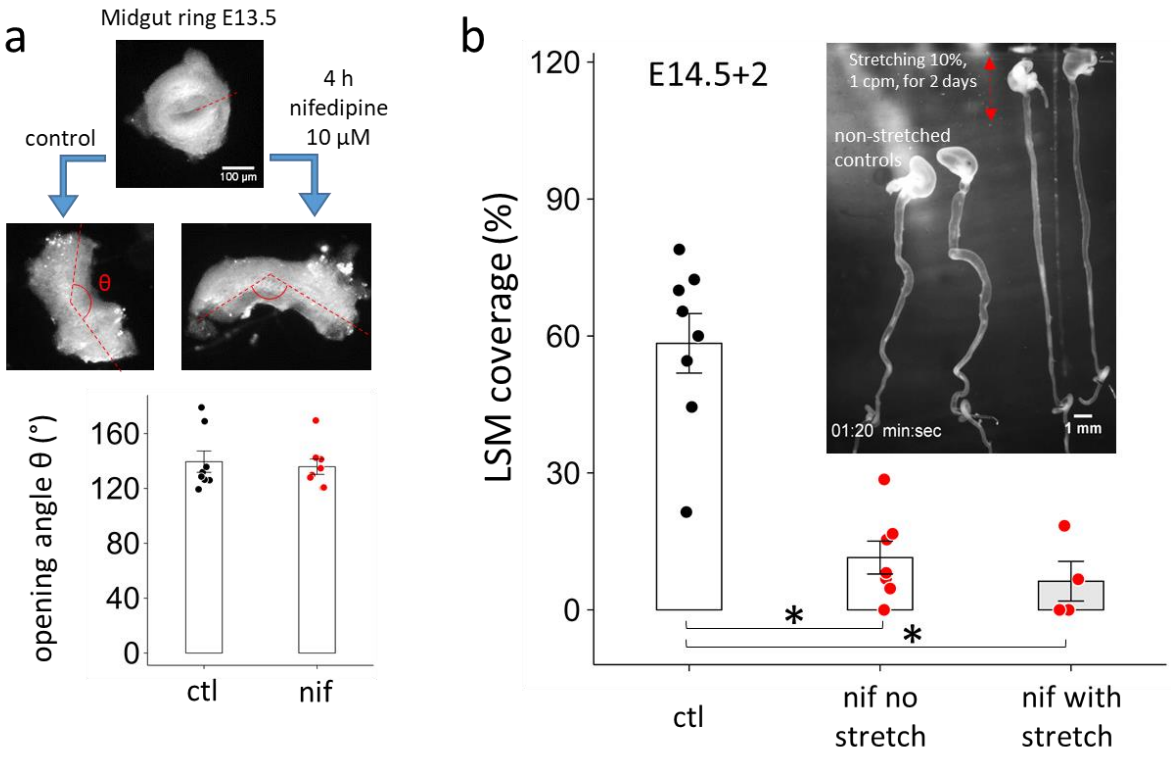

Figure 4. ***Mechanical stimulation does not rescue LSM differentiation inhibition by nifedipine****. (a) Opening angles of E13.5 duodenum of control guts (n=8 rings from n=4 different embryos) and guts treated for 4h in nifedipine 10 uM. Stage E13.5 was chosen because no CSM is present at E12.5, which means nifedipine cannot alter contractility at this stage. (b) LSM coverage of E14.5+2 controls (no stretch, no nifedipine, n=8), nifedipine-treated but not stretched (n=7), and nifedipine-treated with a 1 cpm 5-10% external longitudinal stretch (n=4). Inset: experimental setup showing 2 non-stretched guts (left) and 2 stretched guts (right) in the nifedipine-containing trough. The stomachs in the upper right corner are attached to a motor-controlled glass fiber, and pinned at their lower extremity (lower right corner).*

Mesenchymal cells treated with L-type calcium channel blockers remain undifferentiated in early embryos but differentiate to Interstitial cells of Cajal at later stages

We finally asked whether the mesenchymal cells that are inhibited from becoming smooth muscle by L-type channel blockers could differentiate to other cell types. We first analyzed mRNA transcript levels of SM markers ACTA2, ACTG2 and TGLN by RTqPCR in pre-CSM E5 and post-CSM E5+3 chicken embryonic guts. ACTA2 and ACTG2 respectively encode αSMA and γSMA , whereas TGLN encodes SM22, an actin-binding protein. As expected, at E5, the intestinal mesenchymal is not yet

differentiated. We observed an induction of SM markers after 3 days of culture in control conditions (Fig.5a-c). The expression of ACTG2 (Fig.5b) was significant, but the increase for ACTA2 (Fig.5a) and TGLN (Fig.5c) was not. The induction of SM markers was associated with the downregulation of LIX1 (Fig.5d), indicating the commitment of mesenchymal progenitors towards the SMC lineage. Interestingly, this commitment was impaired by nicardipine treatment (Fig.5a-d) as we observed lower levels of ACTA2, ACTG2 and TGLN while LIX1 expression was upregulated compared to control condition (although to a much lesser degree than at E5). KIT mRA levels (Fig.5e) characteristic of Interstitial cells of Cajal (ICC-lineage) were increased in the nicardipine group, but not significantly at these early developmental stages. We used a c-kit antibody commercially available in mice (but not chicken) to assess ICC development at later stages in mice (Fig.5f-h). We found that nifedipine-treated samples at E14.5 exhibited a distinct population of c-kit expressing cells (Fig.5g,h), that were not or only sparsely found in controls (Fig.5f,h). c-kit expressing cells were found mostly at the level of the myenteric plexus, between the CSM and presumptive LSM layers (Fig.5g); a few c-kit positive cells were also present in the epithelium. These results indicate that the inhibition of smooth muscle differentiation by nifedipine leads to an increased commitment of mesenchymal cells towards an ICC phenotype in mice.

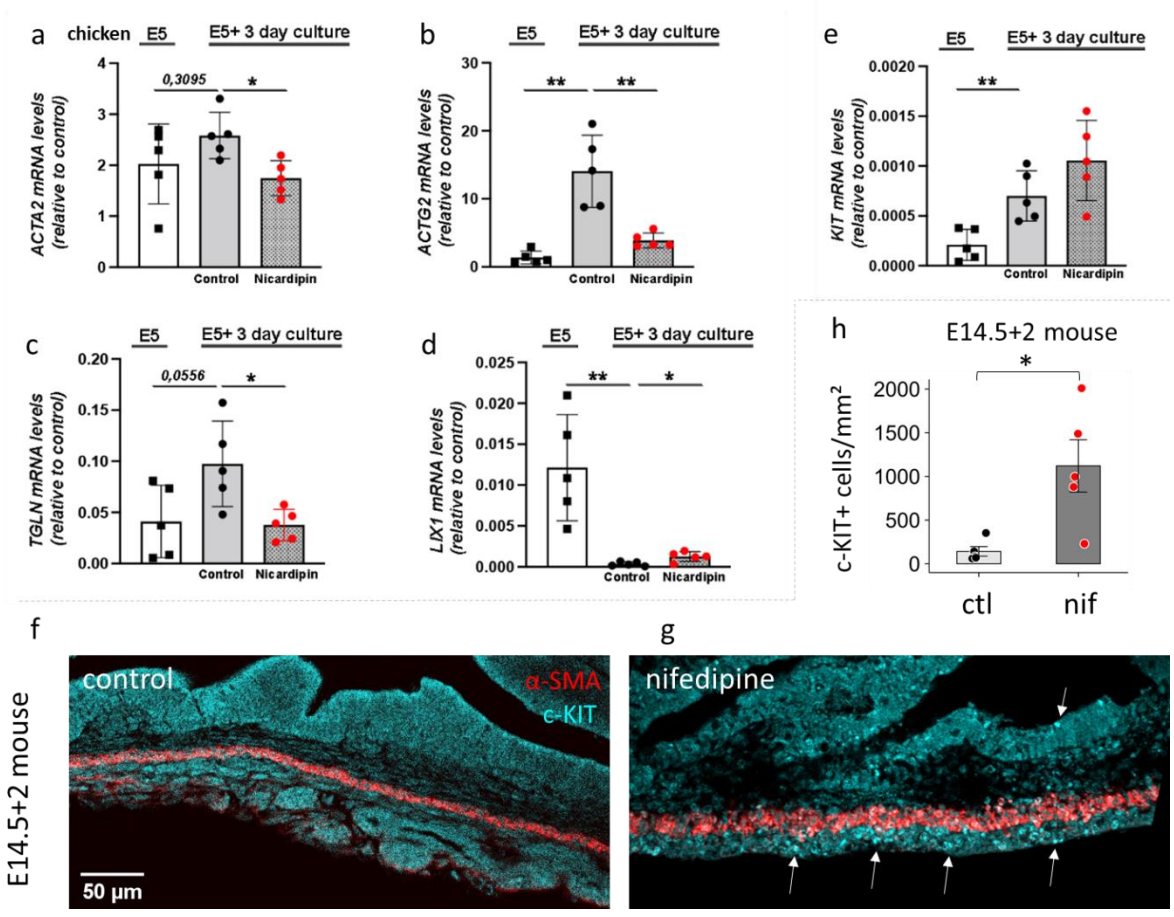

Figure 5. ***What happens to the smooth muscle differentiation inhibited mesenchyme*** *? (a-e) Quantification of transcript levels by RT-quantitative PCRs in control and nicardipine treated chicken embryonic guts at E5, E5+3 days of culture. Data were normalized to GAPDH and 60S acidic ribosomal protein P0 (RPLPO) expression. Values are presented as the mean SD of n=5 for each condition. (f,g) SMA and c-KIT immunohistochemistry of E14.5+2 mouse duodenum control and nifedipine-treated samples. White arrows point at c-KIT positive ICCs. (h) c-KIT positive cells per mm² mesenchyme in control (n=5) and 10 µM nifedipine treated (n=5) E14.5+2 gut. Each dot corresponds to a different sample. *P < 0.05 and **P < 0.01 by 2-tailed Mann-Whitney tests.*

Discussion

In this study, we showed that L-type calcium channel sensitive calcium waves propagate in the mouse intestinal mesenchyme one day prior to CSM and LSM differentiation (Fig.1). L-type calcium channel antagonists block the mesenchymal calcium waves, inhibit CSM and LSM differentiation, and halt growth of the embryonic organs (Fig.2, Fig.S2). Although we could not pharmacologically dissociate calcium waves from contractility (Fig.3), we found that external mechanical stimulation could not recover smooth muscle differentiation when calcium waves are impaired (Fig.4). Mesenchymal calcium waves therefore directly affect molecular factors responsible for SM differentiation, rather than through a mechanobiological effect mediated by SM contraction. L-type calcium channel blockers caused early embryonic mesenchyme to partially remain in a stem-like state, overexpressing the *LIX1* factor, while later fetal mesenchymal cells over-differentiated to ICCs instead of smooth muscle (Fig.5).

Our findings echo several recent discoveries on the role of calcium waves in drosophila wing (Brodskiy et al., 2019), chicken feather bud (Li et al., 2018) and mouse limb (Atsuta et al., 2019) development. An important question is how the electric depolarization event mediated by calcium waves leads to expression of markers responsible for differentiation to a given cell type. Cytoplasmic Ca^{2+} ions entering through voltage gated calcium channels can act as an intracellular second messenger, activating several downstream signals, such as the calmodulin (CaM)/calcineurin and the PKC/MAPK pathways (Atsuta et al., 2019). This in turn might modulate important molecular signals for smooth muscle differentiation, such as the Shh or the BMP pathways (Huycke et al., 2019; Mao et al., 2010) - modulation of Shh by cell bioelectric activity has in fact been demonstrated in chicken feather budding (Li et al., 2018). An integrated picture of cell differentiation in organs will obviously require connecting the biomechanical, bioelectrical, and biomolecular events that take place in the embryo. It is also presently unclear what parameters of the depolarization event – frequency, amplitude, duration - are important for the control of differentiation. Our experiment with the L-type channel agonist Bay K8644 showed that it had complex effects on calcium waves, first increasing their amplitude and duration, but then leading to short, low-amplitude, higher-frequency wave trains and eventually a global decrease of calcium activity. Consistent with these observations, application of this compound in culture led to a decrease of CSM differentiation.

We found that inhibition of calcium waves and contractions by L-type calcium channel blockers also impeded embryonic gut growth. These results extend to a mammalian model previous conclusions by our group (Chevalier, 2022; Chevalier et al., 2018; Khalipina et al., 2019) on the essential role of CSM contractility in gut lengthening and morphogenesis. We found here that CSM contractility is necessary right from the start of CSM differentiation (E12.5 in mice, E5 in chicken) for further intestinal growth. The YAP1 pathway mediates the proliferative response of the mouse intestinal tissue in response to mechanical stress (Yang et al., 2021), but the role of contractions had been sidelined by these investigators, based on the fact that intestinal culture in the Rho inhibitor Y-27632 did not prevent gut growth: here we show that this inhibitor does not actually affect embryonic CSM contractility (Fig.3e-g). We recently realized that virtually all gut growth defects observed in animal mutants in the literature are coupled with smooth muscle impediments (Chevalier, 2022). Together, these facts strongly bolster our view that SM contractility should be regarded as a key factor for gut growth and regeneration in pathologies such as extended gastrointestinal cancer or short-bowel syndrome.

Our work presents some discrepancies with a recent study on smooth muscle orientation during development (Huycke et al., 2019). These investigators reported that 10 µM nifedipine treatment of E9+3 chicken guts led to misorientation of the outer (LSM) muscle layer. They did not however quantitatively report the extent of LSM differentiation along the gut tract. Here, we find that nicardipine not only halts contractions of the CSM, but also prevents to a large extent LSM (Fig.S1h-j).

Our results are consistent with results showing that nifedipine reduced the extent of smooth muscle differentiation in the developing mouse lung bud (Goodwin et al., 2019). Huycke et al. also found that proper LSM orientation could be recovered by cyclic longitudinal stretch in the late chicken embryo when subject to nifedipine. We find that a similar cyclic longitudinal stretch procedure in the mouse embryo does not lead to any LSM differentiation. This discrepancy could be related to species differences, or to the fact that only orientation was reported by Huycke et al., and not the extent of LSM differentiation along the gut tract.

It is classically understood that contractility in skeletal and smooth muscle is triggered by Ca^{2+} entry through voltage gated channels and the subsequent release of calcium from intracellular stores. Two pathways are activated by this increase in intracellular Ca^{2+}: on the one hand calmodulin that activates MLCK, on the other hand RhoA-Rho kinase that inhibits MLCP. MLCK and inhibited MLCP jointly lead to phosphorylation of MLC20 that initiates actin-myosin stepping leading to contraction (Deng et al., 2012; Rattan et al., 2010). We expected that breaking this cascade at the level of MLCK with ML-7 would inhibit contractility, but not upstream calcium-related events. We find that ML-7 does however perturb calcium waves, by reducing their frequency at low concentrations, and by disorganizing the physiological synchrony of the calcium uprise across the mesenchyme at higher concentrations. These results show that the above-described cascade of events is not unidirectional, but that perturbations at any level feedback upstream, perturbing the whole calcium handling chain within the cell. We were also surprised to find that inhibition of Rho with Y-27632 (up to 50 µM) did not affect contractility in the early developing mouse gut. The Rho pathway is known to be involved in adult gut smooth muscle contraction, particularly of its tonic component (Rattan et al., 2010); our results indicates that this pathway is not required for embryonic gut phasic contractility. We had previously found that blebbistatin, a myosin inhibitor, was equally ineffective at halting contractility in the embryonic gut (Chevalier, 2018).

Besides contractile smooth muscle, mesenchymal cells in the gut can also differentiate to pacemaker interstitial cells of Cajal (ICCs), fibroblasts, or blood vessels of the presumptive mucosa. Many gastrointestinal diseases, like chronic intestinal pseudo-obstruction (Der-Silaphet et al., 1998) or diabetes (Chen et al., 2018) are characterized by a lack of intestinal rhythmicity and a depletion of the ICC pool (Chetaille et al., 2014; He et al., 2001; Isozaki et al., 1997). It is therefore of clinical importance to understand how a normal SM-ICC balance can be restored in these pathologies. We found that nifedipine led to a x10 fold increase in c-KIT expressing ICC cells in the intestinal mesenchyme of E14.5+2 mouse embryos. It is well-known that the electric pacemaking activity of ICCs is not dependent on L-type calcium channels (Chevalier et al., 2020; Lee et al., 1999). Here we show that L-type calcium channels are not required for ICC differentiation, and that the concomitant inhibition of SM differentiation by nifedipine brings about a shift towards an ICC phenotype. This effect is similar to that of PDGF receptor blocking, which inhibits LSM differentiation and instead triggers ICC differentiation at the outer gut periphery (Kurahashi et al., 2008). Recently, we showed that PDGFRA expression was associated to CIPO SMCs (Martire et al., 2021) due to a phenotypic switch of the CIPO-SMC towards undifferentiated stage. At earlier embryonic stages, we showed that LIX1 was upregulated and SM22 downregulated in nicardipine-treated samples, suggesting that the intestinal mesenchyme remained undifferentiated. The capacity of gastrointestinal, but also vascular and urogenital SMC, to plastically alter their phenotype between a differentiated/contractile and an immature/proliferative phenotype under exogenous or endogenous stimulation can lead to important functional alterations (Le Guen et al., 2015; Scirocco et al., 2016).

Nifedipine and nicardipine are commonly used smooth-muscle relaxing drugs to treat hypertension during pregnancy, a disorder that occurs in 2-3% of pregnancies (Davis et al., 2011). Because many

pregnancies are unexpected, the fetus may also inadvertently exposed to these drugs during the first trimester (Magee et al., 1996). Nifedipine crosses the placenta (Ferguson et al., 1989). Our study suggests that the sustained use of these drugs during early pregnancy could affect smooth muscle differentiation of the embryo. We did not come across any studies reporting increased malformation associated to nifedipine intake during the first trimester, and could in particular not find any mention of lower gastrointestinal tract ailments associated to *in-utero* nifedipine exposure (Davis et al., 2011; Fitton et al., 2017; Magee et al., 1996; Malha and August, 2019; Smith et al., 2000; Sørensen et al., 2001). It is likely that the benefit of lower blood pressure during pregnancy outweighs the risks linked to teratogenic effects of L-type calcium channel blockers, which have so far only been reported in animal models at higher and sustained concentrations (Scott et al., 1997), such as in the present study.

Materials and Methods

Ethics

All experiments were performed in accordance with the ethics guidelines of the INSERM and CNRS.

Mouse gut samples

The Cre reporter mice C57BL/6N-Gt(ROSA)26Sor^{tm1}(CAG-GCaMP6f)Khakh/J mice, referred to as Gcamp6fl/fl, were obtained from The Jackson Laboratory (Stock No: 029626). A transgenic mouse line in which the transgene is under the control of the 3-kb fragment of the human tissue plasminogen activator (Ht-PA) promoter Tg(PLATcre) 116Sdu16, was referred as Ht-PA::Cre. GCamp6fl/fl males were crossed with Ht-PA::Cre females to generate embryos carrying the calcium fluorescent reporter in neural crest cells and their derivatives. In approximately ~25% of the embryos, the GCamp6f signal was located in the mesenchyme, but not in the NCCs. These mesenchyme-specific GCamp6f reporter mice were used for calcium imaging in this study; neural-crest specific GCamp6f expressing guts were used for culture experiments. For some experiments where the GCamp6f reporter was not required, we also used wildtype C57Bl/6N mice from the animal husbandry of the Institut Jacques Monod (Paris). Animals were dissected at stages E11.5-E14.5, embryos removed, and the gut of each embryo was dissected in PBS from stomach to colon.

Chicken gut samples

Fertilized chicken eggs were purchased from EARL Morizeau (Chartres, France, breeder Hubbard, JA57 hen, I66 rooster, yielding type 657 chicks). The eggs were incubated at 37.5 °C in a humidified chamber for 5 to 10 days. The gastrointestinal tracts were dissected from stomach to hindgut, the mesentery and Remak's nerve were removed.

Calcium imaging and analysis

After dissection, each gut was immobilized in 1 mL of 1% low-melting point agarose (Sigma A4018) in a 35 mm diameter Petri dish (Greiner), and covered with 4 mL of DMEM:F12 Glutamax (Gibco 31331-028) with 1% penicillin-streptomycin and 15 mM HEPES. Guts were imaged on a thermostated support at 36.5±1°C on a Zeiss LSM 780 upright confocal microscope with a x20 objective, at illumination wavelength 488 nm, fluorescence was collected in the range 492-630 nm, at a 2 Hz acquisition rate. Some videos were also acquired on an inverted spinning disk confocal microscope (Olympus). Drugs were added from stock solutions directly in the Petri dish under the microscope and homogenized by up-down movements with a 1 mL pipette. The effect of each drug concentration was assessed for at least 3 min. Analysis of calcium waves were performed by drawing a region-of-interest (ROI) over the

regions (either the presumptive CSM or LSM), and plotting the pixel intensity against time; we computed the frequency as the number of intensity peaks per unit time extracted from 3-5 min videos, and the average intensity ratio as the average I_{peak} / $I_{baseline}$ for all peaks, but using the Matlab "findpeaks" function.

Organotypic culture and morphometrics

E12.5 and E13.5 mouse guts were cultured in DMEM:F12 Glutamax (Gibco ref 31331-028) 1% penicillin-streptomycin in individual 35 mm diameter Greiner culture dishes, and cultured for 2 to 3 days in a humidified incubator at 37°C, in a 5% CO_2 – 95% air atmosphere. For bulkier E14.5 guts the atmosphere was 5% CO_2 – 95% O_2. The length of the guts was measured prior to and post-cultures from binocular images (MZ series, Leica) with the ImageJ "segmented line" function. E5 and E10 chicken guts were cultured in 1 mL DMEM with 1% penicillin-streptomycin in 35 mm diameter Greiner culture dishes, and cultured for 72 h in a humidified incubator at 37°C, in a 5% CO_2 – 95% air atmosphere.

Cyclic stretch culture

Cyclic stretch culture was performed in a 40 mL optically transparent trough covered with a vertical sheet of PDMS (~5 mm thick). Control E14.5 (non-stretched) guts were pinned at the stomach and caecum to the PDMS sheet, without applying stretch. The stomach of the stretched E14.5 guts was first attached to a thin (~0.5 mm) horizontal glass fiber obtained by heat-pulling a Pasteur pipette. The caecum was then pinned to the PDMS in such a way that the gut was fully elongated (but not stretched) in the vertical direction. The Pasteur pipette was fastened to a micro-stepper motor (Newport M-UTM linear stage with ESP300 controller), controlled via an RS232 interface and a Matlab program. Each stretch cycle corresponded to a 2-3 mm upward movement of the glass fiber (to which the stomachs are attached) at a speed of 2 mm/sec, a 2 sec pause in the stretched state, and a subsequent downward movement of 2-3 mm at 2 mm/sec back to the initial state. The strain computed from $(l_{stretched} - l_{relaxed})/l_{relaxed}$ was in the range 5-10%. The stretch was applied at 1 cycle per minute, corresponding approximately to the frequency of spontaneous CSM contractions in the mouse gut (Chevalier et al., 2021b). Because this cyclic stretch gradually increased the length of the intestine, we repositioned the upper fiber 2 times per day to correct for this**.** Guts were harvested after 48h and processed for IHC as described below.

Opening angle measurements

E13.5 mouse guts were divided and cultured for 4h in medium in DMEM:F12 Glutamax containing either only vehicle (control), or nifedipine 10 µM. After this incubation, two rings ~0.5 mm long were cut from the proximal midgut and cut open longitudinally along one of the gut walls with microscissors. This operation was performed on a heated plate at 37°C, in the incubation medium. The morphology of the ring post-cutting was imaged with a binocular and the resulting opening angle measured with ImageJ.

Monitoring of Gut Motility

Spontaneous motility of chicken and mice gut post-culture was monitored by placing them in 1 mL of medium in individual dishes at 37°C and time-lapse imaging with a binocular (MZ series, Leica) and camera (Stingray) at a 1 Hz frequency for 2 min. Space-time diagrams of motility (Chevalier *et al.*, 2017) in different regions were extracted with the imageJ "Reslice" function.

Immunohistochemistry

Post-culture samples were fixed for 1 h in 4% PFA in PBS, washed 3 times, then blocked and permeated in 1% BSA and 0.1% triton in PBS overnight, immersed in 1:500 α-SMA Cy3 conjugated antibody (Sigma C6198) and 1:500 βIII-tubulin FITC conjugated antibody (ab224978) for 24h, washed, immobilized in 1% agarose gel (Sigma A4018) in PBS and imaged (Zeiss LSM 780). For assessment of the percent fraction of gut length covered by CSM or LSM we imaged the gut along the midgut length from proximal duodenum to the ileo-caecal junction and we computed the ratio of length where these muscular layers were present over the total midgut length.

For KIT IHC, samples were dehydrated for 24 h in 30% sucrose solution in water, and embedded in OCT. Frozen sections were performed on a Leica cryotome at 20 µm thickness. Section were blocked and permeated in 1% BSA and 0.1% triton in PBS overnight, incubated with a c-KIT-AF647 conjugated antibody (1:100, Santa Cruz Biochemicals sc-393910) overnight, washed, and imaged.

Quantitative real-time RT-PCR

Total RNA was extracted from cultured intestines with the HighPure RNA Isolation Kit (Roche). Reverse transcription (RT) were performed using the Verso cDNA Synthesis Kit (Thermo Scientific) and quantitative real time PCR was performed using the LightCycler technology (Roche Diagnostics). PCR primers (Table S1) were designed using the LightCycler Probe Design software-2.0. Four individual intestines were individually analyzed for each conditions. Levels of *KIT, LIX1, αSMA, SM22* and *SOX10* transcripts were determined with the LightCycler analysis software (version 3.5) relative to standard curves. Data were presented as the expression levels *of KIT, LIX1, αSMA, SM22* and *SOX10* relative to the expression of the reference genes GAPDH and RPLPO. The relative mRNA expression was calculated using the 2-ΔΔCT method (Faure et al., 2015; McKey et al., 2016).

Statistics and Reproducibility

All sample numbers indicated in this report correspond to different embryos (guts, biological replicates). For mice, information was collected from at least 2 different litters per age. All experiments involving culture were technically replicated at least twice, i.e. they were performed on two different days with fresh samples following the same procedure each time. A minimum of n=4 samples constitutes each group presented in this report. Statistical analysis was performed with the two-tailed Mann-Whitney test and was considered significant at $p<0.05$.

Acknowledgments

This research was funded by the Agence Nationale de la Recherche ANR GASTROMOVE - ANR-19-CE30-0016-01, by the Université de Paris IDEX Emergence en Recherche CHEVA19RDX-MEUP1, by the CNRS PEPS INSIS “COXHAM” grant, by the Labex “Who AM I ?”, and by the Imaging platform BioEmergences-IBiSA, ANR-10-INBS-04 and ANR-11-EQPX-0029. We are grateful to Sylvie Dufour for providing us with the Ht-PA::Cre mouse line.

Author contributions

NRC led the project, obtained funding, performed experiments, analyzed data, synthesized data; PdSB and SF performed experiments and analyzed data; LZ, AG, RAA, LP, ILP, NR, IA performed experiments; NRC, PdSB and SF wrote the paper.

References

Amedzrovi Agbesi, R. J. and Chevalier, N. R. (2021). Gastrointestinal hydrodynamics: flow and mixing induced by slow waves. *Phys. Rev. Fluids* **submitted**,.

Atsuta, Y., Tomizawa, R. R., Levin, M. and Tabin, C. J. (2019). L-type voltage-gated Ca2+ channel CaV1.2 regulates chondrogenesis during limb development. *Proc. Natl. Acad. Sci. U. S. A.*

Brodskiy, P. A., Wu, Q., Soundarrajan, D. K., Huizar, F. J., Chen, J., Liang, P., Narciso, C., Levis, M. K., Arredondo-Walsh, N., Chen, D. Z., et al. (2019). Decoding Calcium Signaling Dynamics during Drosophila Wing Disc Development. *Biophys. J.* **116**, 725–740.

Chen, Y., Wang, H., Li, H. and Liu, S. (2018). Long-pulse gastric electrical stimulation repairs interstitial cells of cajal and smooth muscle cells in the gastric antrum of diabetic rats. *Gastroenterol. Res. Pract.* **2018**,.

Chetaille, P., Preuss, C., Burkhard, S., Côté, J.-M., Houde, C., Castilloux, J., Piché, J., Gosset, N., Leclerc, S., Wünnemann, F., et al. (2014). Mutations in SGOL1 cause a novel cohesinopathy affecting heart and gut rhythm. *Nat. Genet.* **46**, 1245–1249.

Chevalier, N. R. (2018). The first digestive movements in the embryo are mediated by mechanosensitive smooth muscle calcium waves. *Philos. Trans. R. Soc. B Biol. Sci.* **373**, 1759.

Chevalier, N. (2022). Physical organogenesis of the gut. *Development* **149**, dev200765.

Chevalier, N. R., de Witte, T.-M., Cornelissen, A. J. M., Dufour, S., Proux-Gillardeaux, V. and Asnacios, A. (2018). Mechanical Tension Drives Elongational Growth of the Embryonic Gut. *Sci. Reports 2018 81* **8**, 1–10.

Chevalier, N. R., Ammouche, Y., Gomis, A., Teyssaire, C., de Santa Barbara, P. and Faure, S. (2020). Shifting into high gear: how Interstitial Cells of Cajal change the motility pattern of the developing intestine. *Am. J. Physiol. Liver Physiol.* **319**, G519–G528.

Chevalier, N., Amedzrovi-Agebsi, R., Ammouche, Y. and Dufour, S. (2021a). How smooth muscle contractions shape the developing enteric nervous system. *Front. Cell Dev. Biol.* **accepted**,.

Chevalier, N. R., Ammouche, Y., Gomis, A., Langlois, L., Guilbert, T., Bourdoncle, P. and Dufour, S. (2021b). A neural crest cell isotropic-to-nematic phase transition in the developing mammalian gut. *Commun. Biol.* **4**, 770.

Davis, R. L., Eastman, D., McPhillips, H., Raebel, M. A., Andrade, S. E., Smith, D., Yood, M. U., Dublin, S. and Platt, R. (2011). Risks of congenital malformations and perinatal events among infants exposed to calcium channel and beta-blockers during pregnancy. *Pharmacoepidemiol. Drug Saf.* **20**, 138–145.

de Santa Barbara, P., Williams, J., Goldstein, A. M., Doyle, A. M., Nielsen, C., Winfield, S., Faure, S. and Roberts, D. J. (2005). Bone morphogenetic protein signaling pathway plays multiple roles during gastrointestinal tract development. *Dev. Dyn.* **234**, 312–322.

Deng, M., Deng, L., Xue, Y., Deng, M., Deng, L. and Xue, Y. (2012). MAP Kinase-Mediated and MLCK-Independent Phosphorylation of MLC20 in Smooth Muscle Cells. *Curr. Basic Pathol. Approaches to Funct. Muscle Cells Tissues - From Mol. to Humans*.

Der-Silaphet, T., Malysz, J., Hagel, S., Arsenault, A. L. and Huizinga, J. D. (1998). Interstitial cells of Cajal direct normal propulsive contractile activity in the mouse small intestine. *Gastroenterology* **114**, 724–36.

Faure, S., McKey, J., Sagnol, S. and de Santa Barbara, P. (2015). Enteric neural crest cells regulate vertebrate stomach patterning and differentiation. *Development* **142**, 331–42.

Ferguson, J. E., Schutz, T., Pershe, R., Stevenson, D. K. and Blaschke, T. (1989). Nifedipine pharmacokinetics during preterm labor tocolysis. *Am. J. Obstet. Gynecol.* **161**, 1485–1490.

Fitton, C. A., Steiner, M. F. C., Aucott, L., Pell, J. P., Mackay, D. F., Fleming, M. and McLay, J. S. (2017). In-utero

exposure to antihypertensive medication and neonatal and child health outcomes: a systematic review. *J. Hypertens.* **35**, 2123.

George, L. F. and Bates, E. A. (2022). Mechanisms Underlying Influence of Bioelectricity in Development. *Front. Cell Dev. Biol.* **10**, 1–17.

Goodwin, K., Mao, S., Guyomar, T., Miller, E., Radisky, D. C., Košmrlj, A. and Nelson, C. M. (2019). Smooth muscle differentiation shapes domain branches during mouse lung development. *Dev.* **146**,.

He, C. L., Soffer, E. E., Ferris, C. D., Walsh, R. M., Szurszewski, J. H. and Farrugia, G. (2001). Loss of interstitial cells of Cajal and inhibitory innervation in insulin-dependent diabetes. *Gastroenterology* **121**, 427–434.

Huizinga, J. D., Chen, J. H., Zhu, Y. F., Pawelka, A., McGinn, R. J., Bardakjian, B. L., Parsons, S. P., Kunze, W. A., Wu, R. Y., Bercik, P., et al. (2014). The origin of segmentation motor activity in the intestine. *Nat. Commun.* **5**, 3326.

Huycke, T. R., Miller, B. M., Gill, H. K., Nerurkar, N. L., Sprinzak, D., Mahadevan, L. and Tabin, C. J. (2019). Genetic and Mechanical Regulation of Intestinal Smooth Muscle Development. *Cell* **179**, 90-105.e21.

Isozaki, K., Hirota, S., Miyagawa, J., Taniguchi, M., Shinomura, Y. and Matsuzawa, Y. (1997). Deficiency of c-kit+ cells in patients with a myopathic form of chronic idiopathic intestinal pseudo-obstruction. *Am. J. Gastroenterol.* **92**, 332–4.

Khalipina, D., Kaga, Y., Dacher, N. and Chevalier, N. (2019). Smooth Muscle Contractility Causes the Gut to Grow Anisotropically. *J. R. Soc. Interface* **16**, 20190484.

Kurahashi, M., Niwa, Y., Cheng, J., Ohsaki, Y., Fujita, A., Goto, H., Fujimoto, T. and Torihashi, S. (2008). Platelet-derived growth factor signals play critical roles in differentiation of longitudinal smooth muscle cells in mouse embryonic gut. *Neurogastroenterol. Motil.* **20**, 521–531.

Le Guen, L., Marchal, S., Faure, S. and De Santa Barbara, P. (2015). Mesenchymal-epithelial interactions during digestive tract development and epithelial stem cell regeneration. *Cell. Mol. Life Sci.* **72**, 3883–3896.

Lee, J. C. F., Thuneberg, L., Berezin, I. and Huizinga, J. D. (1999). Generation of slow waves in membrane potential is an intrinsic property of interstitial cells of Cajal. *Am. J. Physiol. - Gastrointest. Liver Physiol.* **277**, G409-23.

Li, A., Cho, J. H., Reid, B., Tseng, C. C., He, L., Tan, P., Yeh, C. Y., Wu, P., Li, Y., Widelitz, R. B., et al. (2018). Calcium oscillations coordinate feather mesenchymal cell movement by SHH dependent modulation of gap junction networks. *Nat. Commun.* **9**, 1–15.

Magee, L. A., Schick, B., Donnenfeld, A. E., Sage, S. R., Conover, B., Cook, L., McElhatton, P. R., Schmidt, M. A. and Koren, G. (1996). The safety of calcium channel blockers in human pregnancy: A prospective, multicenter cohort study. *Am. J. Obstet. Gynecol.* **174**, 823–828.

Malha, L. and August, P. (2019). Safety of Antihypertensive Medications in Pregnancy: Living With Uncertainty. *J. Am. Heart Assoc.* **8**,.

Mao, J., Kim, B., Rajurkar, M., Shivdasani, R. and McMahon, A. (2010). Hedgehog signaling controls mesenchymal growth in the developing mammalian digestive tract. *Development* **137**, 1721–1729.

Martire, D., Garnier, S., Sagnol, S., Bourret, A., Marchal, S., Chauvet, N., Guérin, A., Forgues, D., Berrebi, D., Chardot, C., et al. (2021). Phenotypic switch of smooth muscle cells in paediatric chronic intestinal pseudo-obstruction syndrome. *J. Cell. Mol. Med.* **25**, 4028–4039.

McHugh, K. M. (1995). Molecular analysis of smooth muscle development in the mouse. *Dev. Dyn.* **204**, 278–290.

McKey, J., Martire, D., de Santa Barbara, P. and Faure, S. (2016). LIX1 regulates YAP1 activity and controls the proliferation and differentiation of stomach mesenchymal progenitors. *BMC Biol.* **28**, 14–34.

Opie, L. H. (1997). Pharmacological differences between calcium antagonists Calcium channel structure and binding sites. *Eur. Heart J.* **18**, 71–79.

Ramalho-Santos, M., Melton, D. A. and McMahon, A. P. (2000). Hedgehog signals regulate multiple aspects of gastrointestinal development. *Development* **127**, 2763–2772.

Rattan, S., Phillips, B. R. and Maxwell IV, P. J. (2010). RhoA/Rho-Kinase: Pathophysiological and Therapeutic Implications in Gastrointestinal Smooth Muscle Tone and Relaxation. *Gastroenterology* **138**, 13.

Roberts, R. R., Ellis, M., Gwynne, R. M., Bergner, A. J., Lewis, M. D., Beckett, E. A., Bornstein, J. C. and Young, H. M. (2010). The first intestinal motility patterns in fetal mice are not mediated by neurons or interstitial cells of Cajal. *J. Physiol.* **588**, 1153–1169.

Scirocco, A., Matarrese, P., Carabotti, M., Ascione, B., Malorni, W. and Severi, C. (2016). Cellular and Molecular Mechanisms of Phenotypic Switch in Gastrointestinal Smooth Muscle. *J. Cell. Physiol.* **231**, 295–302.

Scott, W. J., Resnick, E., Hummler, H., Clozel, J. P. and Bürgin, H. (1997). Cardiovascular alterations in rat fetuses exposed to calcium channel blockers. *Reprod. Toxicol.* **11**, 207–214.

Shimizu, H., Koizumi, O. and Fujisawa, T. (2004). Three digestive movements in Hydra regulated by the diffuse nerve net in the body column. *J. Comp. Physiol. A Neuroethol. Sensory, Neural, Behav. Physiol.* **190**, 623–630.

Sicard, P., Falco, A., Faure, S., Thireau, J., Lindsey, S. E., Chauvet, N. and de Santa Barbara, P. (2022). High-resolution ultrasound and speckle tracking: a non-invasive approach to assess in vivo gastrointestinal motility during development. *Development* **149**, dev200625.

Smith, P., Anthony, J. and Johanson, R. (2000). Nifedipine in pregnancy. *Br. J. Obstet. Gynaecol.* **107**, 299.

Sørensen, H. T., Czeizel, A. E., Rockenbauer, M., Steffensen, F. H. and Olsen, J. (2001). The risk of limb deficiencies and other congenital abnormalities in children exposed in utero to calcium channel blockers. *Acta Obs. Gynecol Scand* **80**, 397–401.

Uhlén, P. and Fritz, N. (2010). Biochemistry of calcium oscillations. *Biochem. Biophys. Res. Commun.* **396**, 28–32.

Wallace, A. S. and Burns, A. J. (2005). Development of the enteric nervous system, smooth muscle and interstitial cells of Cajal in the human gastrointestinal tract. *Cell Tissue Res.* **319**, 367–382.

Yang, Y., Paivinen, P., Xie, C., Krup, A. L., Makela, T. P., Mostov, K. E. and Reiter, J. F. (2021). Ciliary Hedgehog signaling patterns the digestive system to generate mechanical forces driving elongation. *Nat. Commun. 2021 121* **12**, 1–14.

Supplementary Information to

“Mesenchymal calcium waves underpin intestinal smooth muscle differentiation“

Nicolas R. Chevalier, Léna Zig, Anthony Gomis, Richard J. Amedzrovi, Laetitia Pontoizeau, Isabelle Le Parco, Nathalie Rouach, Isabelle Arnoux, Pascal de Santa Barbara, Sandrine Faure

Video S1 : E12.5 pre-CSM waves in jejunum and the inhibiting effect of nifedipine 10 µM

Video S2 : Pre-LSM and CSM waves in the hindgut of E13.5+1

Video S3 : Calcium chirping in pre-LSM cells at the outer periphery of E14.5 duodenum

Video S4 : Calcium activity is low at E11.5 in the cecum but increases as the cecum buds in culture

Video S5 : Dose effect of ML-7 on E12.5 pre-CSM waves

Video S6 : Y27632 10 µM does not inhibit contractility in E12.5+2 cultures, and also when the concentration is increased for 1 h to 50 µM.

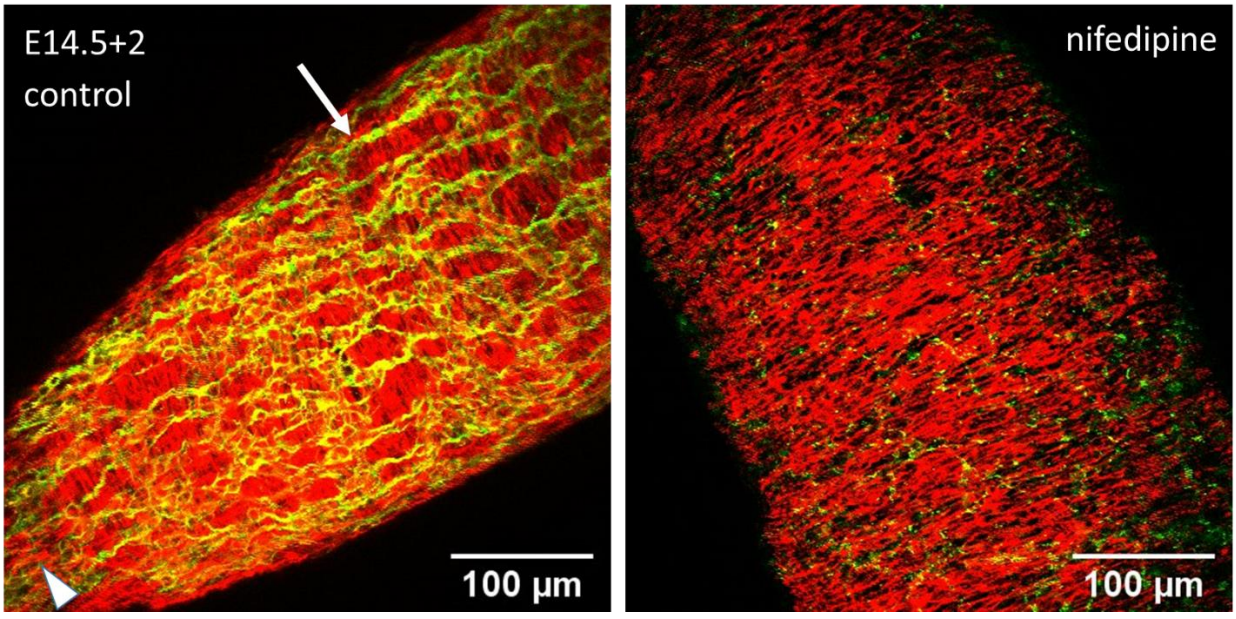

Figure S1. Maximum projection confocal z-stack of E14.5+2 samples, α-SMA in red, neuronal Tuj in green, in control (left) and nifedipine 10 µM (right) conditions. Note the presence of the LSM in the control (only visible in the lower left corner because of the projection, white arrowhead) and of a well-formed ENS mesh network (white arrow). No LSM is present with nifedipine and the ENS network is degraded, but the CSM layer is intact.

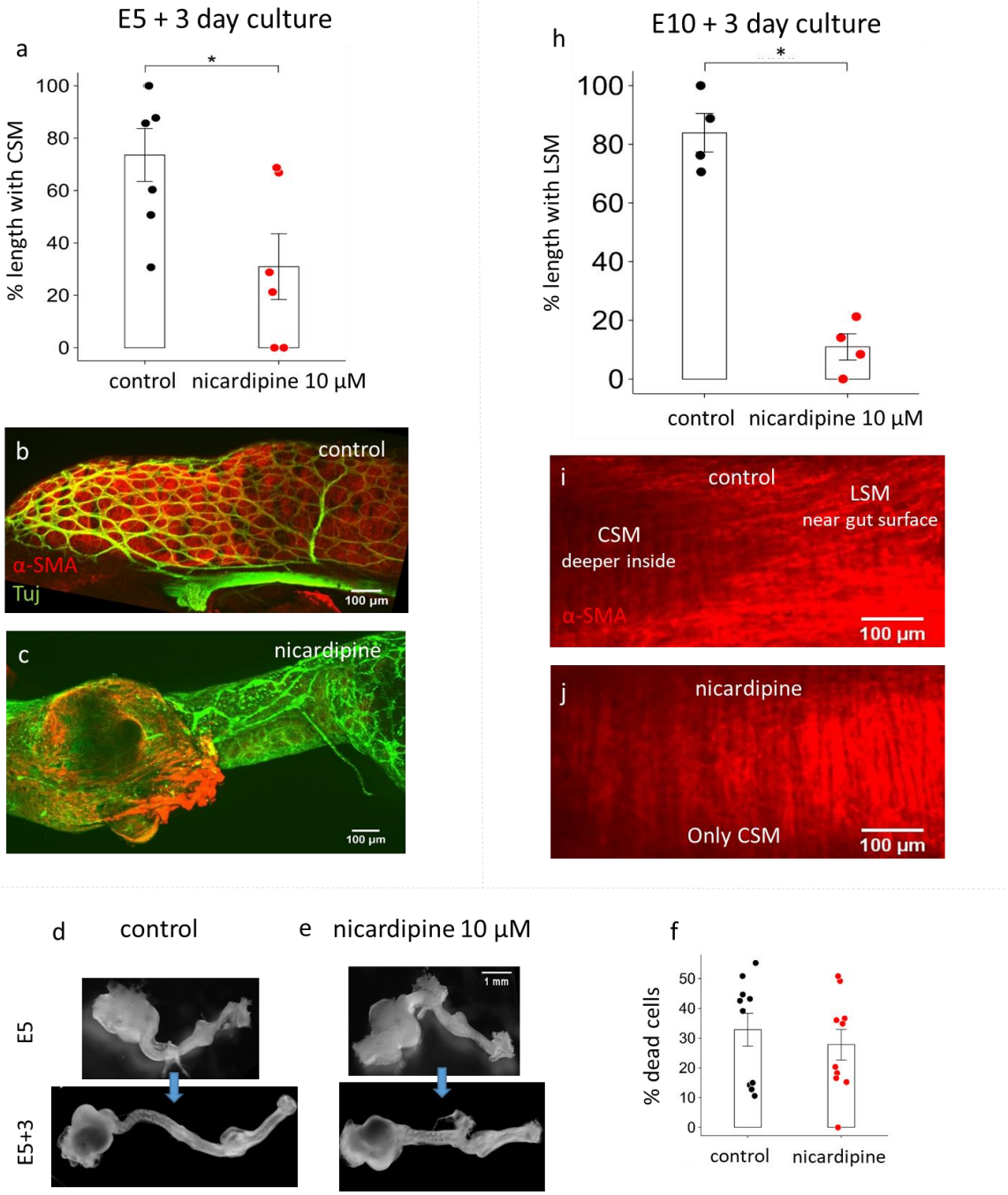

Figure S2. ***L-type calcium channel blockers inhibit CSM & LSM differentiation and growth of chicken embryonic guts.*** *(a) CSM coverage of chicken E5+3 control (DMSO vehicle alone 1:1000) and nicardipine-treated samples. (b,c) Maximum projection confocal z-stack of control and nicardipine-treated E5+3 samples, α-SMA in red, neuronal Tuj in green. (d,e) Representative morphological evolution after 3 day culture of (d) control and (e) nicardipine treated E5 chicken gut. Scale bar indicated in the upper right panel is the same for all pictures. (f) Length increased of E5+3 chicken gut compared to before culture at E5. (d) LSM coverage of chicken E10+3 gut control and nicardipine-treated samples. (e,f) Maximum projection confocal z-stack of control and nicardipine-treated E10+3 samples, α-SMA in red. * p<0.05, Mann-Whitney two-tailed test. Each dot represents a different sample.*

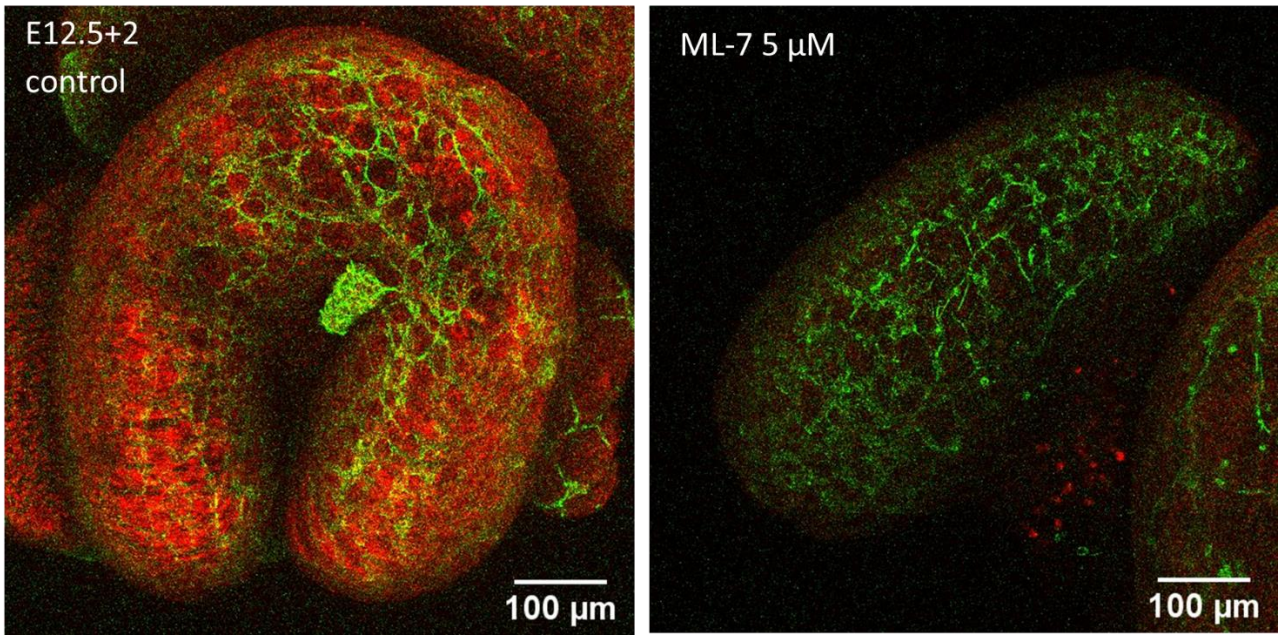

Figure S3. Maximum projection confocal z-stack of control and ML-7 treated E12.5+2 samples, α-SMA in red, neuronal Tuj in green, in control (left) and nifedipine 10 µM (right) conditions. In ML-7 5 µM, CSM differentiation is abolished (this sample) or reduced, but the ENS forms a similar mesh network as in controls.